

XII. QUE94201

Basalt, 12 grams

Weathering Be



Figure XII-1. Photograph illustrating broken interior surface of Martian meteorite QUE94201. Scale is in mm. (NASA # S96-00376)

Introduction

Five sides of QUE94201 are rounded and polished with remnant fusion crust, while one side appears freshly broken (figure XII-1). The interior is coarse-grained, crystalline and glassy (Score and Mason 1995). “Mafic-rich areas” (probably shock-melted glass), as large as 5 x 4 mm, were noted during preliminary examination. In thin section, the sample is made up of subequal amounts of homogeneous maskelynite laths and variable interstitial pyroxene. Maskelynite laths are up to 3.6 mm long.

QUE94201 is a basalt apparently similar to the dark, mottled lithology (DML) of Zagami (McSween *et al.* 1996) as well as “lithology B” of EETA 79001 (Mikouchi *et al.* 1998). However, the phosphorous content of QUE94201 is high and the REE pattern is strongly depleted in light rare earth elements. The extreme zoning in pyroxene in QUE94201 indicates that it cooled quickly from magmatic temperatures. The Fe-Ti oxide compositions indicate that this basalt formed under more

reducing conditions than the other shergottites (McSween *et al.* 1996; Herd *et al.* 2001d; Kring *et al.* 2003).

A recent review of QUE94201 by Kring *et al.* (2003) relates QUE94201 to the lherzolitic shergottites, because of the LREE depletion, but notes that it was a basaltic liquid before it crystallized. Warren *et al.* (1999) find that QUE94201 is very low in Ni and Ir content.

Petrography

Harvey *et al.* (1996) described QUE94201 as a “coarse-grained basalt, consisting of subhedral Fe-rich pigeonite and maskelynite”. Kring *et al.* (2003) note that it was a “bulk melt”, meaning that its composition can be used to infer the magmatic source region. Most of the pyroxene and maskelynite grains exceed 1 mm in length (up to 3 mm) and are somewhat elongated (figures XII-2; XII-7). QUE94201 contains relatively high proportions of maskelynite and phosphate when

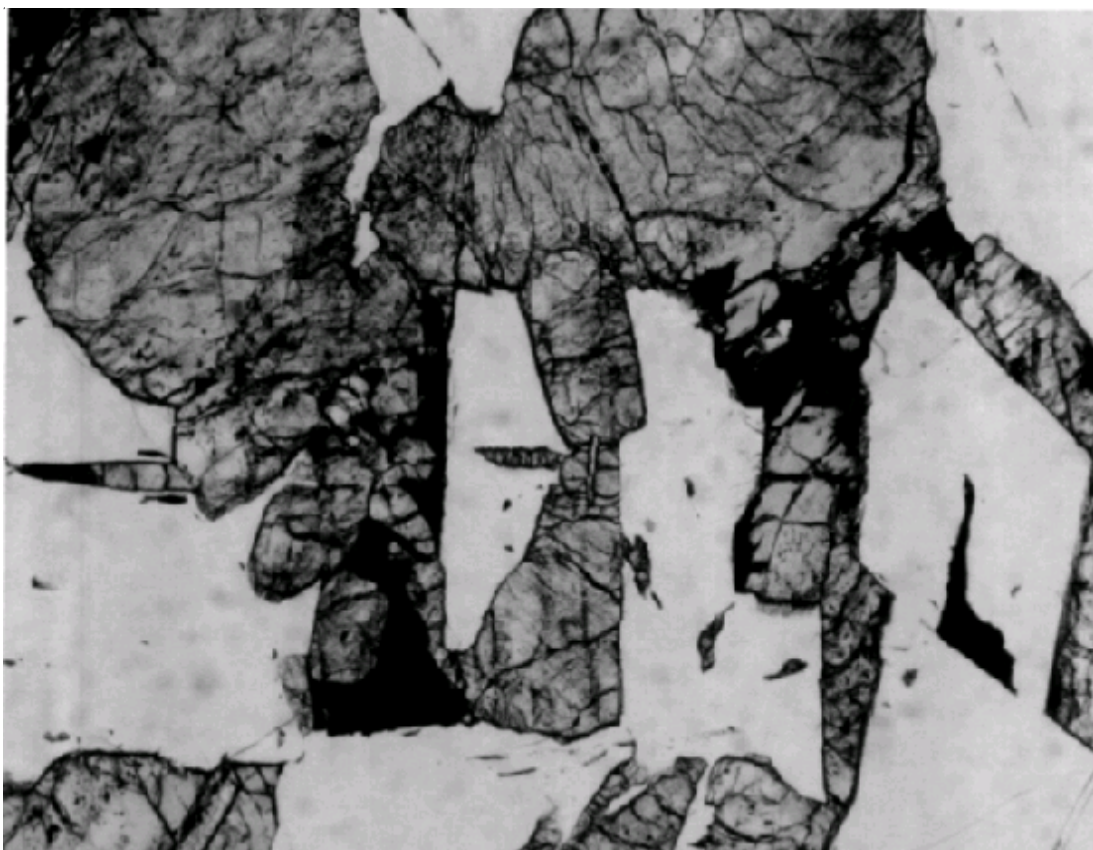


Figure XII-2. Photomicrograph of thin section of QUE94201,4 illustrating basaltic texture. Field of view is 2.2 mm.

compared with the other shergottites. Melt inclusions are found in the relict plagioclase (Kring *et al.* 2003) but no melt inclusions were found in the pyroxene.

The pyroxenes in QUE94201 are complexly zoned (McKay *et al.* 1996; Mikouchi *et al.* 1996; 1998 and McSween and Eisenhour 1996). The Mg-rich pigeonite cores are mantled by Mg-rich augite, which is, in turn, rimmed by Fe-rich pigeonite and strongly zoned to pyroxferroite (with some hedenbergite at the edge). None of the cores appear to be cumulate phases, as was the case for Shergotty, Zagami and EETA79001B. Some of the pyroxenes in QUE94201 are also found to be sector zoned.

Interstitial to the pyroxene and shocked plagioclase, are

a number of late-stage phases including large Fe-Ti oxides (ulvöspinel, rutile, ilmenite), whitlockite and large “pockets” of mesostasis similar to the “DN pockets” of Zagami (McCoy *et al.* 1995). These “pockets” contain an intergrowth of silica and fayalite, as well as, maskelynite, whitlockite, Fe-Ti oxides, sulfides, minor augite, chlorapatite and a Zr-rich phase, probably baddelyite (McSween *et al.* 1996). Fayalite-silica intergrowths are also found in the cores of large skeletal phosphate grains adjacent to these pockets (Harvey *et al.* 1996). Aramovich *et al.* (2002) have carefully studied the symplectite intergrowths associated with merrillite grains in QUE94201 and conclude that the early formation of Ca and Mg-rich merrillite lead to the formation of metastable pyroxferroite and ferrosilite, which then broke down to become the fine-grained intergrowths.

Shock features include maskelynite, mosaicism in pyroxene and large pockets of glass formed *in-situ*. The shock-melted glass is rich in phosphorous (Mikouchi *et al.* 1998).

Mineralogical Mode for QUE94201

	Harvey <i>et al.</i> (1998)	Mikouchi <i>et al.</i> (1996)
Pyroxene	44 vol. %	43
Maskelynite	46	42
Opaque	2	4
Phosphate	4	6
Mesostasis	4	5

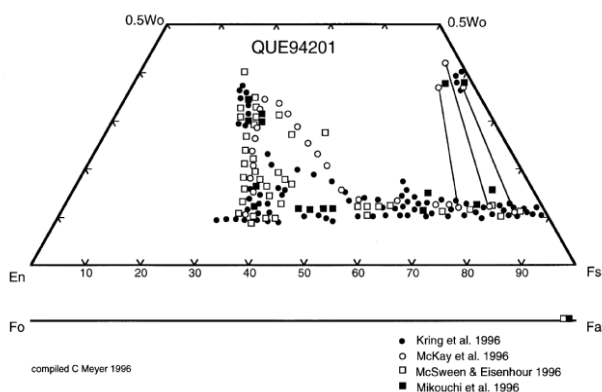


Figure XII-3. Composition diagram for pyroxene and olivine in QUE94201. Data are from Kring *et al.* (1996), McKay *et al.* (1996), McSween and Eisenhower (1996) and Mikouchi *et al.* (1996). Olivine is pure fayalite.

Mineral Chemistry

Pyroxene: Pyroxene zoning is extreme (figures XII-3; XII-8), including sector zoning in the cores (Kring *et al.* 1996; Mikouchi *et al.* 1996, 1998; McKay *et al.* 1996; McSween and Eisenhower 1996). Harvey *et al.* (1996) report pigeonite zoning to Fs_{85} . Wadhwa and Crozaz (1996), McSween *et al.* (1996) and Wadhwa *et al.* (1998) have determined the REE patterns of the pyroxenes and suggested that merrillites began crystallizing relatively early. The Eu anomaly indicates reducing conditions.

“Pyroxferroite”: An analysis of “pyroxferroite” is given in Mikouchi *et al.* (1998), however, Aramovich *et al.* (2002) point out that the reported composition ($Wo_{37}En_3Fs_{60}$) is too Ca-rich for it to be termed “pyroxferroite”.

Maskelynite: Plagioclase (An_{66-52}) crystallized throughout the crystallization sequence (McSween and Eisenhower 1996; Mikouchi *et al.* 1999). The cores are the most An-rich among the basaltic Martian meteorites. It has been shocked to maskelynite. Plagioclase is found to include melt inclusions (Kring *et al.* 2003).

Phosphates: QUE94201 contains more phosphates than other SNC meteorites. Whitlockite (merrillite) has been studied by Wadhwa and Crozaz (1996) and found to have a more extreme depletion of LREE than for any other shergottite. Mikouchi *et al.* (1998) analyzed merrillite up to 3 mm long. Mikouchi *et al.* (1996, 1998), McSween *et al.* (1996) and Leshin *et al.* (1996) also

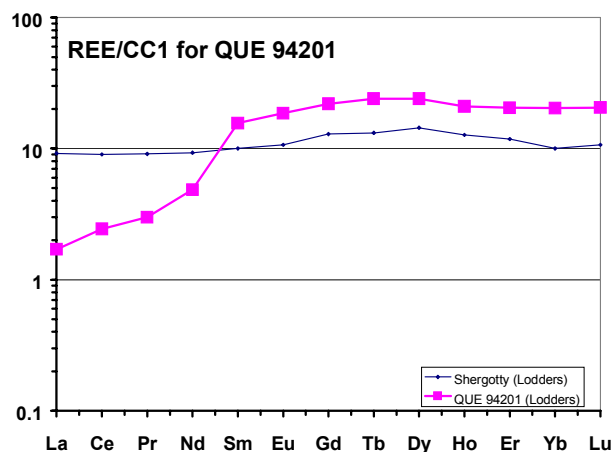


Figure XII-4. Normalized rare earth element diagram for QUE94201 compared with that of Shergotty.

report minor chlorapatite in the mesostasis. Aramovich *et al.* (2002) show that the formation of merrillite is often surrounded by symplectite intergrowths.

Silica: Silica occurs as distinctive intergrowth with fayalite in “patches” up to 1 mm in-between pyroxene and plagioclase grains (Harvey *et al.* 1996). Silica was also reported as an alteration product by Wentworth and Gooding (1991).

Olivine: Fayalite (Fa_{96-99}) occurs as a fine dendritic intergrowth with silica (Harvey *et al.* 1996).

Opagues: Large grains of ilmenite are the major opaque phase. Analyses for ilmenite and ulvöspinel are reported in Kring *et al.* (1996), McSween *et al.* (1996), Mikouchi *et al.* (1998) and Herd *et al.* (2001). Chromite has been found in Mg-rich pigeonite core (Mikouchi *et al.*). Ulvöspinel exhibits subsolidus “oxyexsolution” of ilmenite lamellae on the order of 300-500 nm wide (Herd *et al.*)

Sulfide: The sulfide phase is pyrrhotite (McKay *et al.* 1996; McSween and Eisenhower 1996).

Glass: QUE94201 contains abundant pockets of shock-melted glass. This melt contains up to 7 % P, probably due to preferential melting of the abundant phosphates (Mikouchi *et al.* 1996, 1998). K-poor and K-rich feldspar glasses have also been reported in the mesostasis by Mikouchi *et al.*

Table XII-1a. Chemical composition of QUE94201.

	Warren96		Dreibus96		Kring 96		Kring 96		Mikouchi96		Mittlefehldt 96	Warren 97	
weight	305 mg		179.8 mg		250mg		fusion crust		fusion crust		52.74 mg	305 mg	
SiO ₂ %	47.06	(a)					43.5	(d)	44.3	(d)		48.00	(d)
TiO ₂	1.95	(a)	1.8	(b)	1.7	(b)	1.81	(d)	2	(d)		1.98	(b)
Al ₂ O ₃	9.64	(a)	12	(b)	11.1	(b)	7.46	(d)	7	(d)		9.82	(b)
FeO	18.65	(a)	18.3	(b)	18.3	(b)	24.2	(d)	21	(d)	20.0	19.16	(b)
MnO	0.48	(a)	0.436	(b)	0.44	(b)	0.63	(d)	0.6	(d)		0.47	(b)
CaO	11.3	(a)	11.3	(b)			10.9	(d)	11.2	(d)	10.7	11.48	(b)
MgO	6.3	(a)	6.2	(b)			6.04	(d)	6.4	(d)		6.3	(d)
Na ₂ O	1.39	(a)	1.75	(b)			1.16	(d)	1.1	(d)	1.53	1.39	(b)
K ₂ O	0.038	(a)	0.052	(b)			0.04	(d)				0.04	
P ₂ O ₃							2.77	(d)	3.4	(d)			
sum	96.81						98.51		97			98.64	
Li ppm													
C													
F			40	(b)									
S													
Cl			91	(b)									
Sc	49	(b)	46.6	(b)							51.5	49.0	(b)
V	124	(b)	103	(b)								124	
Cr	1030	(b)	890	(b)								1010	
Co	24.4	(b)	22.8	(b)							25.9	24.4	(b)
Ni	<40	(c)	<20	(b)								<40	
Cu													
Zn	108	(c)									130	108	
Ga	26	(b)	27.1	(b)								25.9	
Ge													
As			0.77	(b)									
Se													
Br			0.35	(b)			Borg 97		Borg 97		0.38		
Rb				(b)			0.518	(f)	0.691	(f)		<6	
Sr	59	(b)	80	(b)			41.3	(f)	49.8	(f)	70	59	
Y			31.2	(e)									
Zr	94	(b)	97.1	(e)							80	94	
Nb			0.68	(e)									
Mo													
Pd ppb													
Ag ppb													
Cd ppb													
In ppb													
Sb ppb													
Te ppb													
I ppm			4.6	(b)									
Cs ppm												<0.12	
Ba	<41	(b)	<15	(b)								<41	
La	0.44	(b)	0.35	(b)							0.31	0.44	
Ce	1.63	(b)	1.3	(b)							1.0	1.63	
Pr							Borg 97						
Nd	2.4	(b)	1.9	(b)			1.482	(f)				2.36	
Sm	2.55	(b)	2.02	(b)			1.233	(f)			1.92	2.55	
Eu	1.09	(b)	0.99	(b)							0.9	1.09	
Gd			4.3	(b)									
Tb	0.93	(b)	0.802	(b)							0.78	0.93	
Dy	6.1	(b)	5.53	(b)									
Ho			1.19	(b)									
Er													
Tm													
Yb	3.5	(b)	3.09	(b)							3.02		
Lu	0.54	(b)	0.455	(b)							0.42	0.54	
Hf	3.4	(b)	3.42	(b)							4.2	3.4	
Ta	<0.08	(b)	0.023	(b)							0.03	<0.08	
W ppb													
Re ppb													
Os ppb													
Ir ppb	<2.4	(b)	<3	(b)								<2.4	
Au ppb			<1.5	(b)								<0.5	
Tl ppb													
Bi ppb													
Th ppm	<0.09	(b)	0.05	(e)								<0.09	
U ppm			0.0125	(e)								<0.2	

technique: (a) emp fused bead, (b) INAA, (c) RNAA, (d) emp, (e) spark source mass spec., (f) isotope dilution mass spec.

Table XII-1b. Chemical composition of QUE94201

reference	Lodders 98	Wang 98	Warren 99	Blichert-Toft 99	Kring 2003				
weight	average		285 mg.	50 mg. 48 mg. 57 mg.	47.4 mg	81.32	125.87	254.6	
SiO ₂	47.9		47.92						
TiO ₂	1.84		1.98	(a)	1.6	1.82	1.67	1.7	(a)
Al ₂ O ₃	11		9.82	(a)	15.17	11.7	10.94	11.98	(a)
FeO	18.5		19.17	(a)	15.37	18.65	18.01	17.73	(a)
MnO	0.45		0.47	(a)	0.38	0.44	0.45	0.44	(a)
CaO	11.4		11.47	(a)	10.77	10.35	10.65	10.63	(a)
MgO	6.25		6.3	(a)	5.47	4.81	6.63	5.8	(a)
Na ₂ O	1.58		1.37	(a)	2.13	1.86	1.79	1.87	(a)
K ₂ O	0.045		0.04	(a)	0.052	0.061	0.077	0.067	(a)
P ₂ O ₅									
sum									
Li ppm									
Sc	48		49	(a)	38.5	45.8	48.8	45.9	(a)
V	113		124	(a)	84	92	104	96	(a)
Cr	950		1010	(a)	792	809	1054	927	(a)
Co	24	13.7	(b) 24.4	(a)	20.22	23.1	24.2	23.1	(a)
Ni	<20		6.6	(b)	150	120	<80	<106	(a)
Cu									
Zn	110	87.4	(b) 90	(b)	65	82	84	80	(a)
Ga	27	20.1	(b) 25.9	(a)	27.6	30.5	25	27.2	(a)
Ge			1.95	(b)					
As	0.77		<0.6						
Se		0.473	(b)		2.9	2.8	1.8	2.3	(a)
Br	0.35		0.5	(a)					
Rb		0.545	(b)		<13		8.4	8.4	(a)
Sr	70		59	(a)					
Y	31								
Zr	100		94	(a)	118	159	107	126	(a)
Nb	0.68								
Mo									
Pd ppb									
Ag ppb		3.46	(b)						
Cd ppb		52.6	(b) <50	(b)					
In ppb		76.7	(b)						
Sb ppb		5.3	(b)						
Te ppb		4.1	(b)						
I ppm	4.6								
Cs ppm		0.032	(b) <0.120	(a)					
Ba	<15								
La	0.4		0.44	(a)	0.35	0.45	0.46	0.44	(a)
Ce	1.47		1.63	(a)	<1.8	1.62	1.19	1.36	(a)
Pr									
Nd	2.2		2.36	(a)	<5	3.8	3.1	3.4	(a)
Sm	2.3		2.55	(a)	1.747	2.53	2.436	2.34	(a)
Eu	1.04		1.09	(a)	1.086	1.208	1.144	1.154	(a)
Gd	4.3								
Tb	0.87		0.93	(a)	0.76	1.034	1.026	0.979	(a)
Dy	5.8		6.1	(a)					
Ho	1.19		1.32	(a)	0.95	1.35	1.23	1.22	(a)
Er									
Tm					0.45	0.58	0.51	0.52	(a)
Yb	3.3		3.5	(a)	2.7	3.77	3.5	3.44	(a)
Lu	0.5		0.54	(a)	0.403	0.389	0.727	(c) 0.383	0.556 0.496 0.494 (a)
Hf	3.41		3.4	(a)	2.99	3.17	4.28	(c) 2.76	3.9 2.61 3.05 (a)
Ta	0.023		<0.08	(a)					
W ppb					<1.1	<0.8	0.54	0.54	(a)
Re ppb			0.0028	(b)	60	42	29	39	(a)
Os ppb			0.0051	(b)					
Ir ppb	<3		0.012	(b)	< 12	6	5	5	(a)
Au ppb	<0.5	0.145	(b) 0.041	(b)	< 7	5	< 4		(a)
Tl ppb		20.9	(b)						
Bi ppb		1.54	(b)						
Th ppm	<0.05		<0.09	(a)					
U ppm	<0.05	0.023	(b) <0.2	(a)					
technique	(a) INAA, (b) RNAA, (c) IDMS								

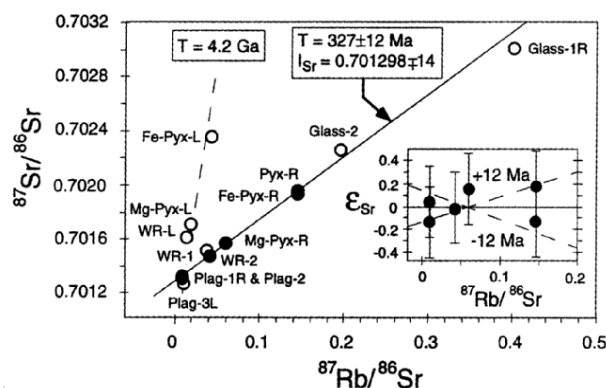


Figure XII-5. Rb-Sr isochron for QUE94201 as reported by Borg *et al.* (1997), GCA **61**, 4920.

Salts: Fe-K-sulfates are sometimes observed rimming Fe-sulfides (Harvey *et al.* 1996). The salts have been studied in detail by Wentworth and Gooding (1996). They found that “carbonates are conspicuously absent.”

Baddelyite: ZrO₂ is reported in the mesostasis (McSween *et al.* 1996).

Whole-rock Composition

The chemical composition of QUE94201 has been determined and reported by Dreibus *et al.* (1996), Warren and Kallemeyn (1996, 1997), Mittlefehldt and Lindstrom (1996), Warren *et al.* (1999) and Kring *et al.* (2003). The sample has very high phosphorous content (table XII-1). This is also reflected in the analysis of the fusion crust and modal mineralogy of the thin sections (Kring *et al.* 1996; Mikouchi *et al.* 1996). Note that Ni and Ir are rather low (6 and 0.012 ppm, Warren *et al.*)(but apparently high in Kring *et al.* 2003).

QUE94201 is a basalt that is greatly depleted in LREE (figure XII-4). Kring *et al.* (2003) make a careful effort to compute the major element composition. Key to this computation is knowledge of P and Si contents as determined from fused bead analyses (Mittlefehldt and Lindstrom 1996) and fusion crust (Kring *et al.* 1996).

Radiogenic Isotopes

Borg *et al.* (1996, 1997) reported a Rb-Sr age ($\lambda_{\text{Rb}} = 1.402 \times 10^{-11} \text{ year}^{-1}$) of $327 \pm 12 \text{ Ma}$ with initial $^{87}\text{Sr}/^{86}\text{Sr}$ ratio of 0.701298 ± 14 (figure XII-5). This low I_{Sr} ratio indicates that the source region (Martian mantle) was depleted in Rb. The Sm-Nd age of 327 ± 19 with $\epsilon_{\text{Nd}} = 47.6 \pm 1.7$ is concordant with the Rb-Sr age

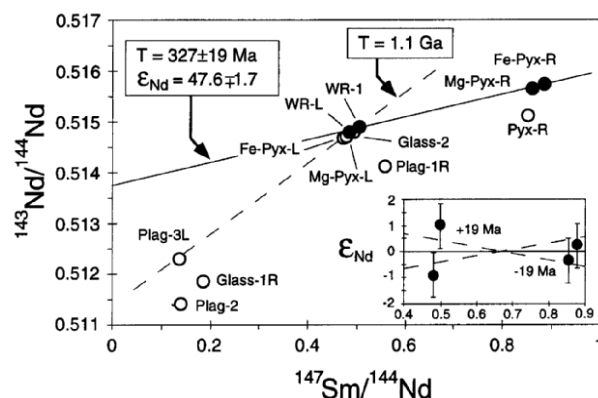


Figure XII-6. Sm-Nd isochron for QUE94201 as determined by Borg *et al.* (1997), GCA **61**, 4921.

(figure XII-6). Dreibus *et al.* (1996b) reported a K/Ar age of 1.33 Ga and Bogard and Garrison (1999) reported 730 Ma by Ar/Ar plateau.

Cosmogenic Isotopes and Exposure Ages

From cosmic-ray produced ^3He , ^{21}Ne and ^{38}Ar , Eugster *et al.* (1996) computed an exposure age for QUE94201 of $2.4 \pm 0.6 \text{ Ma}$ and concluded that QUE94201 was “ejected from Mars simultaneously with the other basaltic shergottites - Shergotty and Zagami”. Nishiizumi and Caffee (1996) found the ^{10}Be concentrations gave a cosmic-ray exposure age of $2.6 \pm 0.5 \text{ Ma}$ for an assumed 4π irradiation geometry. Garrison and Bogard (1998) determined a cosmic ray exposure age of $2.7 \pm 0.6 \text{ Ma}$. Terribillini *et al.* (2000) and Eugster *et al.* (2002) used ^{81}Kr to determine exposure ages of 2.10 ± 0.25 and $2.22 \pm 0.35 \text{ Ma}$ (respectively). Dreibus *et al.* (1996b) and Swindle *et al.* (1996) have also reported exposure ages.

Nishiizumi and Caffee (1996) found that the terrestrial age ($0.29 \pm 0.05 \text{ Ma}$ obtained from ^{36}Cl) of QUE94201 is longer than for other Antarctic shergottites. Jull *et al.* (1997) found that ^{14}C activity was nil, consistent with an old terrestrial age.

Schnabel *et al.* (2001) reported ^{10}Be , ^{26}Al and ^{53}Mn activities of 11.9 ± 0.2 , 63.4 ± 6.9 and $162 \pm 11 \text{ dpm/kg}$ respectively. Kring *et al.* (2003) sum the terrestrial age (0.29 m.a.), with the cosmic ray exposure age (2.6 m.a.) to get an ejection age from Mars of 2.9 m.a.

Other Isotopes

Oxygen isotopes were reported by Clayton and Mayeda (1996) (figure I-3).

Leshin *et al.* (1996, 2000) determined that the hydrogen in six “apatite” grains in QUE94201 has a high D/H ratio ($\delta D = 1700$ to 3500 ‰), probably from the Martian hydrosphere. Boctor *et al.* (2001) also determined the isotopic composition of hydrogen in feldspathic glass.

Grady *et al.* (1996) reported that the carbon released from 450 to 600°C was isotopically light ($\delta^{13}C \sim -24.2$ ‰).

Eugster *et al.* (1996), Swindle *et al.* (1996) and Garrison and Bogard (1998) determined the contents and isotopic ratios of rare gases (Ne, Ar, Kr, Xe) in QUE94201 and found them typical of other shergottites. Small amounts of ^{21}Ne produced by energetic solar protons may be present in QUE94201 (Garrison and Bogard 1998). Garrison and Bogard’s (1998) study was for unmelted mineral phases.

Blichert-Toft *et al.* (1998, 1999) found a very large Hf isotopic anomaly - to match the large Nd and W isotopic anomalies as determined by Borg *et al.* (1997) and Lee and Halliday (1997). *These isotopic anomalies have been preserved in the source region of Martian basalts, since the initial early formation of the crust of Mars!*

Experimental Studies

Since QUE94201 may represent our best example of a primitive basaltic melt (McSween *et al.* 1996), derived from the Martian interior, one can expect numerous experimental studies over the years (*one must accurately know the major element composition*). Mikouchi *et al.* (2001), Koizumi *et al.* (2001), McKay *et al.* (2001) and McCanta and Rutherford (2001) have been trying to reproduce the pyroxenes found in QUE94201 under various fO_2 conditions.

Kring *et al.* (2003) review the “liquid line of descent” on the experimental phase diagrams (Longhi 1991). They note that the bulk composition falls within the olivine stability field rather than on the plagioclase pyroxene liquidus and offer various solutions to this “conundrum”. Experiments that include high phosphorus seem to be needed!

Weathering

Wentworth and Gooding (1996) have studied the weathering products in QUE94201. They report an abundance of Fe-sulfate, but since this is also observed

Table XII-2. Thin sections of QUE94201.

butt	section	2001	parent	picture in
,2			,0	
	,3	Mason		
	,4	MCC		
	,5	McSween		McSween 1996
	,6	Papike		
	,7	Kring		Kring et al. 2003
	,8	Delaney		
	,9	Boctor		
,20			,0	
	,34	Fisk		Mikouchi 1998
	,35	Dreibus		
	,36	Warren		
	,37	Mittlefehldt		
	,38	Terada		
	,46	MCC		

in cavities in the fusion crust, this is almost certainly a weathering product of Antarctic origin (Harvey *et al.* 1996).

Processing

This small sample (12g) has some remnant fusion crust which is difficult to distinguish from interior glass. The sample was initially thought to be a terrestrial rock, but the presence of maskelynite in thin section revealed its Martian origin (confirmed by Fe/Mn and oxygen isotope ratios). Allocations were made from small interior and exterior chips. Two potted butts were used to produce 12 thin sections (table XII-2).

QUE 94201 is listed as a “restricted” sample by the MWG (Score and Lindstrom 1993, page 5) because of its small size.

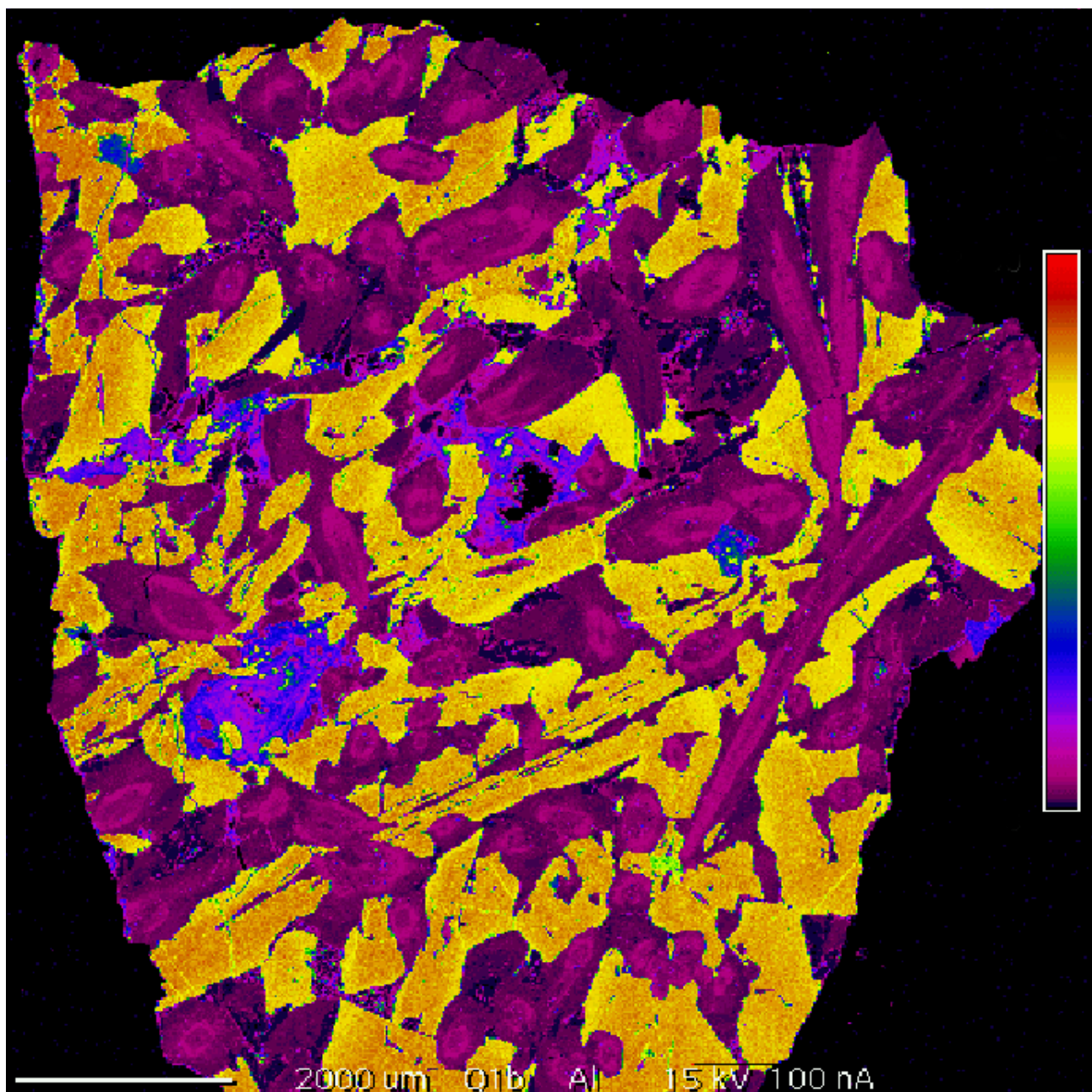


Figure XII-7: X-ray map of whole thin section of QUE 94201. Pink is pyroxene, yellow is maskelynite (figure courtesy of Gordon McKay and Craig Schwandt).

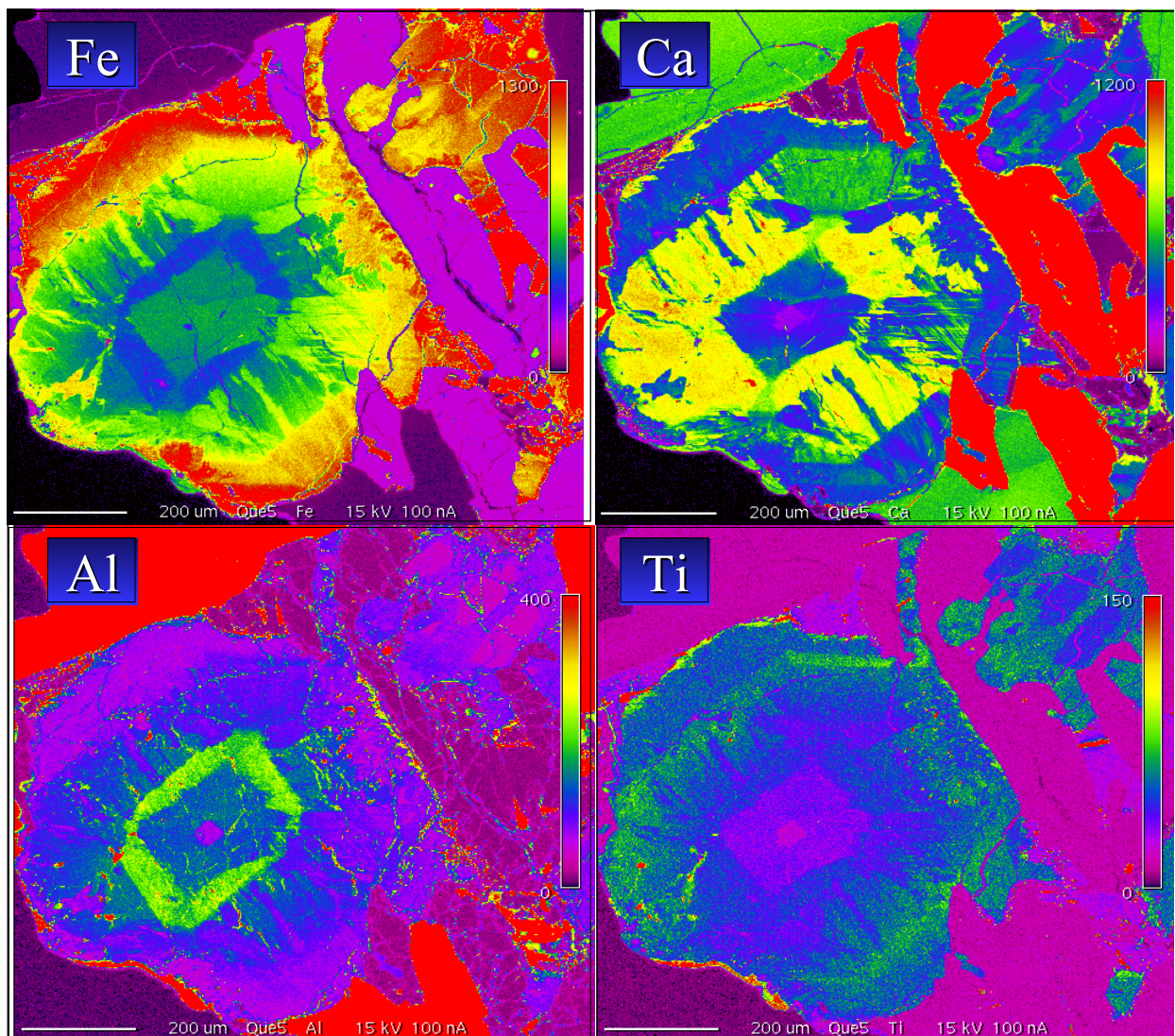


Figure XII-8: X-ray maps of sector-zoned pyroxene in QUE94201 (from bottom left corenr of figure XII-7). (figure courtesy of Gordon McKay and Craig Schwandt).